

Response function and plasmon dispersion for strongly coupled Coulomb liquids: Two-dimensional electron liquid

Kenneth I. Golden

Department of Computer Science and Electrical Engineering, University of Vermont, Burlington, Vermont 05405

G. Kalman

Department of Physics, Boston College, Chestnut Hill, Massachusetts 02167

Philippe Wyns*

Department of Computer Science and Electrical Engineering, University of Vermont, Burlington, Vermont 05405

(Received 29 September 1989)

We employ the recently established formalism for the calculation of the dielectric response function for strongly coupled Coulomb liquids to obtain the dispersion of the plasmon mode in a two-dimensional one-component plasma in the strong-coupling domain. This formalism is based on the physical picture of particles being quasilocalized at strong coupling. The analytical and numerical calculations are carried out over a range of liquid-state coupling parameters up to $\Gamma = e^2\sqrt{\pi n}/k_B T = 120$ and for arbitrary wave numbers. When the slow thermal migration of the quasiparticles (around which the particles are localized) is neglected, the plasmon dispersion is oscillatory and the oscillations become more pronounced with increasing Γ . When the coupling is very strong ($\Gamma = 120$, e.g.), the distance to the first minimum in $\omega(k)$ and the spacing between successive minima approaches $K_0 = 3.3/a$, the lattice spacing in the reciprocal lattice. The "direct" thermal effects due to the slow migration are represented by a phenomenological modification of the dielectric function. This modification leaves the plasmon dispersion almost entirely unaffected up to $ka \approx 1$. For $ka > 1$, however, changes in the dispersion due to the direct thermal motion are as follows: (i) the dispersion is no longer oscillatory; $\omega(k)$ rises from zero to a maximum and then cuts off beyond that at a value $k = k_{\max}(\Gamma)$, which approaches an asymptotic limit $k_{\max}(\Gamma_m)$ close to K_0 as Γ approaches $\Gamma_m = 137 \pm 15$; (ii) the plasmon frequency is increased especially at the lower coupling values where one expects the thermal motion to play a more significant role; (iii) the dispersion exhibits two branches: the upper branch corresponds to the plasmon mode and the heavily damped lower soundlike branch is already identified in random-phase-approximation calculations. We compare our theoretical results with data available from molecular-dynamics (MD) simulations: the agreement between theory and MD data becomes more and more favorable, as it should, with increasing Γ . At $\Gamma = 50$, the agreement is very good indeed.

I. INTRODUCTION

This paper addresses the problem of longitudinal plasma oscillations in a two-dimensional electron liquid consisting of electrons trapped in surface bound states at the interface of dielectric materials. Such a system is well represented by a classical two-dimensional (2D) one-component plasma (OCP) (with $1/r$ interaction) model. One customarily defines the coupling parameter for such systems as $\Gamma = \beta e^2/a$, where e is the renormalized charge which incorporates the effects of the dielectric substrate, $\beta^{-1} = k_B T$, and a , defined through $\pi n a^2 = 1$, is the 2D Wigner-Seitz radius.

It is known from 2D molecular-dynamics (MD) computer simulations¹ that the character of the plasma oscillations, in particular the plasmon dispersion $\omega(k)$, is strongly affected by Γ . For weak coupling ($\Gamma \rightarrow 0$), the random-phase-approximation (RPA) description holds (although it has been theoretically established^{2,3} that, in contrast to the 3D situation, the collisional contributions

in a 2D system are never completely negligible) and with the neglect of thermal effects provides the well-known

$$\omega(k) = \omega_p(k) \equiv (2\pi n e^2 k / m)^{1/2}$$

dispersion with the characteristic \sqrt{k} dependence. The inclusion of thermal effects within the RPA leads to the appearance of $O(k^{3/2})$ terms in the small- k domain and to the development of a maximum⁴ in $\omega(k)$ at $k/\kappa \approx 0.275$ ($\kappa = 2\pi n e^2 \beta$ is the 2D Debye wave number). The thermal RPA model, however, ceases to be a valid description of the 2D plasmon dispersion even for Γ values as low as $\Gamma = 2.29$, the lowest coupling value reported in the molecular-dynamics experiments of Totsuji and Kakeya.¹ As Γ increases, the MD data indicate that starting with $\Gamma = 2.29$ the plasmon frequency changes from slightly above $\omega_p(k)$ to below $\omega_p(k)$ for $\Gamma = 7.09$. For $\Gamma = 23.0, 50.9$, and 70.9 , the plasmon frequency does not change appreciably.

RPA calculations carried out by Platzman and Tzoar⁴ have established the qualitative features of the 2D

plasmon dispersion. This approach, however, has the obvious defect that correlational effects are left out while their importance is indicated by the MD data as discussed above. Theoretical attempts to describe 2D plasmon dispersion for $\Gamma \gtrsim 1$ started with extending the RPA model into the strong-coupling regime.⁴ Studart and Hipolito⁵ employed the static mean-field theory, originally developed for the 3D electron gas by Singwi *et al.*,⁶ to generate local field corrections. Golden and Lu⁷ developed a more sophisticated approach based on the dynamical mean-field theory of Golden and Kalman.⁸ The 2D OCP is known⁹ to crystallize at $\Gamma_m = 137 \pm 15$ into a hexagonal Wigner lattice: the dispersion relation for the crystalline state has been calculated by Bonsall and Maradudin¹⁰ using the conventional harmonic approximation. The Studart-Hipolito⁵ static mean-field theory fails to satisfy the crucially important ω^{-4} sum rule [see Eq. (4) below]; as a consequence, their calculations, if continued beyond their $\Gamma_{\max} = 3.16$ up to $\Gamma \rightarrow \Gamma_m$, would fail to reproduce the correct $k \rightarrow 0$ longitudinal phonon dispersion of Bonsall and Maradudin.¹⁰ This latter defect does not appear in the dynamical mean-field-theory calculation⁷ which is restricted, however, to the $k \rightarrow 0$ domain.

The plasmon dispersion calculation presented in this paper is based on a formalism recently developed by two of us¹¹ (referred to as paper I) for strongly coupled Coulomb liquids. The formalism is based on the physical model of quasilocated particles occupying randomly located sites and undergoing oscillations around them; at the same time, however, the site positions also change and a continuous rearrangement of the underlying quasiequilibrium configuration takes place. Inherent in this model is the assumption that the two time scales are well separated and that for the description of the fast oscillating motion, the time average—converted into ensemble average—of the drifting quasiequilibrium configuration is sufficient. The dielectric function $\epsilon(\mathbf{k}\omega)$ developed on the basis of this physical model is presented in I, Eq. (35), and is displayed here:

$$\epsilon(\mathbf{k}\omega) = 1 - \frac{\omega_p^2(k)}{\omega^2 - \omega_p^2(k)\mathcal{D}(\mathbf{k})}.$$

$\mathcal{D}(\mathbf{k})$, which is given in terms of the equilibrium pair correlation, is defined in Eq. (2) below.

Broadly speaking, the present work consists of two parts. In the first part (Sec. II), we summarize the analysis of the dispersion relation $\epsilon(\mathbf{k}\omega) = 0$ based on I, Eq. (35), and we complete that analysis by carrying out numerical calculations leading to dispersion curves. These curves are compared with the available data from MD simulations¹ of the 2D OCP. We contend that our result is probably the best representation of the plasmon dispersion relation for $\Gamma > 5$ (the explanation of this limiting value is given below; see also paper I) and for arbitrary k values. The dispersion relation in the $\Gamma \rightarrow \Gamma_m$ limit goes over to the Bonsall-Maradudin plasmon dispersion¹⁰ and, for $7 < \Gamma < \Gamma_m$, it is in good agreement with the MD data. To further improve the theoretical description, we develop a phenomenological model to

take into account the part of the thermal effect that corresponds to the slow migration of the random quasites, referred to as the “direct” thermal effect. This is accomplished in the second part of this work (Sec. III) by putting the dielectric response function in a form appropriate for the description of local field corrections⁶

$$\epsilon(\mathbf{k}\omega) = 1 + \frac{\alpha_0(\mathbf{k}\omega)}{1 - \alpha_0(\mathbf{k}\omega)G(\mathbf{k})},$$

where α_0 is the RPA polarizability and $G(\mathbf{k})$ is the “local field correction” which we then identify with $-\mathcal{D}(\mathbf{k})$ of I, Eq. (35). That the dielectric function so constructed has all the desired properties, is discussed in Sec. III. We then analyze this formula and carry out numerical calculations leading to dispersion curves which are again compared with the same MD simulation data and with the dispersion curves obtained in Sec. II. The agreement with the MD data is again quite satisfactory, especially at the higher coupling values $\Gamma = 22, 36, 50$. It is not in this comparison, however, where any real improvement is claimed. Rather, it is in the observation that the structure of the dielectric response function and of the plasmon dispersion is dramatically altered by the inclusion of “direct” thermal effects. In their absence the plasmon dispersion exhibits oscillatory behavior. In their presence the dispersion is no longer oscillatory; it exhibits but one maximum and then cuts off beyond that at a wave-number value $k = k_{\max}(\Gamma)$ which increases with increasing Γ to an asymptotic value $k_{\max}(\Gamma_m)$ close to the lattice spacing in the reciprocal lattice. As to the overall character of $\epsilon(\mathbf{k}\omega)$, there results a marked improvement in the behavior of the static $\epsilon(\mathbf{k}0)$ for small- Γ or high- k values.

Our calculation does not provide any information concerning the damping of plasma oscillations, which in the high- Γ domain is probably primarily due to nonlinear plasmon-plasmon interactions. This process is not described by our model (for a more detailed discussion of this point the reader is referred to paper I), and has to be the subject of a separate investigation.

II. PLASMON DISPERSION WITHOUT DIRECT THERMAL EFFECT

In this section we analyze the dispersion of the 2D OCP plasmon mode in the strong-coupling regime ($7 < \Gamma \leq 120$) for arbitrary wave numbers. We start from Eq. (35) of I for the dielectric response function

$$\epsilon(\mathbf{k}\omega) = 1 - \frac{\omega_p^2(k)}{\omega^2 - \omega_p^2(k)\mathcal{D}(\mathbf{k})} \quad (1)$$

of a 2D Coulomb liquid modeled as described in the Introduction and in paper I; note the absence of “direct” thermal effects in (1). The correlational effects are represented through

$$\begin{aligned}
\mathcal{D}(\mathbf{k}) &= \frac{1}{A} \sum_{\mathbf{q}} \frac{(\mathbf{k} \cdot \mathbf{q})^2}{k^3 q} [g(\mathbf{k} - \mathbf{q}) - g(\mathbf{q})] \\
&= \frac{1}{k^3} \int d^2 r g(r) [1 - \cos(\mathbf{k} \cdot \mathbf{r})] (\mathbf{k} \cdot \nabla) \frac{1}{2\pi r} \\
&= \frac{1}{2k} \int_0^\infty dr \frac{1}{r^2} g(r) \left[1 - 4J_0(kr) + 6 \frac{J_1(kr)}{kr} \right]; \quad (2)
\end{aligned}$$

A is the area of the system and

$$g(r) = \frac{1}{A} \sum_{\mathbf{q}} g(\mathbf{q}) e^{i\mathbf{q} \cdot \mathbf{r}} = \frac{1}{N} \sum_{\mathbf{q}} [S(\mathbf{q}) - 1] e^{i\mathbf{q} \cdot \mathbf{r}}$$

is the equilibrium pair correlation function [see also Eq. (7) of I]. This latter of course depends on the temperature and, in this sense, "indirect" temperature effects are an essential part of our description. Note, finally, that $\mathcal{D}(\mathbf{k})$ is real, and thus, as discussed in the Introduction, cannot describe damping. Equations (1) and (2) are valid for arbitrary values of k .

At high frequencies, Eq. (1) becomes

$$\epsilon(\mathbf{k}\omega \rightarrow \infty) = 1 - \frac{\omega_p^2(k)}{\omega^2} - \frac{\omega_p^4(k)}{\omega^4} \mathcal{D}(\mathbf{k}) - \dots, \quad (3)$$

in agreement with the exact sum rule expansion

$$\epsilon(\mathbf{k}\omega \rightarrow \infty) = 1 - \frac{\omega_p^2(k)}{\omega^2} - \frac{\omega_p^4(k)}{\omega^4} \left[\frac{3ka}{2\Gamma} + \mathcal{D}(\mathbf{k}) \right] - \dots \quad (4)$$

when

$$3ka/(2\Gamma) < \mathcal{D}(\mathbf{k}). \quad (5)$$

For $k \rightarrow 0$, condition (5) suggests that the present theory gives a good approximation for about $\Gamma > 5$.

In the static limit, $\epsilon(k \rightarrow 0, 0)$ provides a negative compressibility sum rule coefficient characteristic of the strongly-coupled state. The absolute value of the coefficient, however, deviates from the exact isothermal compressibility.

The dispersion relation $\epsilon(\mathbf{k}\omega) = 0$ gives

$$\omega(\mathbf{k}) = \omega_p(k) [1 + \mathcal{D}(\mathbf{k})]^{1/2}. \quad (6)$$

We have calculated $\mathcal{D}(\mathbf{k})$ from (2) for arbitrary values of k using $g(r)$ data from (i) the Monte Carlo simulations for $\Gamma = 7.07, 15.81, 22.36,$ and 50 of Totsuji;¹² (ii) the Ref. 13 Monte Carlo simulations for $\Gamma = 36$ and 90 of Gann, Chakravarty, and Chester;¹³ and (iii) the hypernetted chain (HNC) calculations for $\Gamma = 120$ of Ref. 13. Dispersion curves are displayed in Figs. 1(a) and 1(b) with the dimensionless frequency $\bar{\omega}$ and wave number \bar{k} defined as $\bar{\omega} = \omega/\omega_0$, $\bar{k} = ka$; $\omega_0 = (2\pi n e^2 / ma)^{1/2}$. We now turn to a detailed analysis and description of the dispersion curves.

For $k \rightarrow 0$,

$$\mathcal{D}(k \rightarrow 0) \rightarrow \frac{5}{16} \frac{\beta E_c}{n\Gamma} ka, \quad (7)$$

where the correlation energy density E_c is given by the liquid-phase Monte Carlo formula¹²

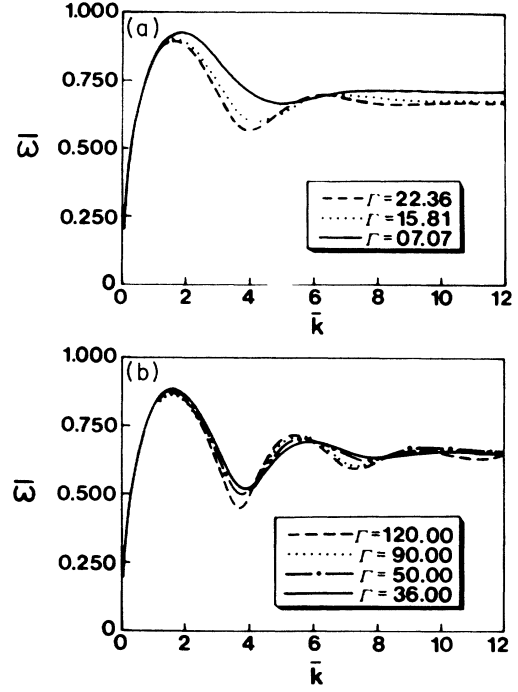


FIG. 1. Plasmon dispersion calculated from Eq. (6) for $\Gamma = 7.07, 15.81, 22.36, 36, 50, 90,$ and 120 ; $\bar{\omega} = \omega/\omega_0$, $\bar{k} = ka$, where $\omega_0 = (2\pi n e^2 / ma)^{1/2}$ and $a = 1/(\pi n)^{1/2}$.

$$\frac{\beta E_c}{n} = -1.12\Gamma + 0.71\Gamma^{1/4} - 0.38 \quad (8)$$

for $\sqrt{2} < \Gamma < 50$, or by the HNC formula¹⁴

$$\frac{\beta E_c}{n} = -1.095\Gamma + 0.985 \quad (9)$$

for $\Gamma > 30$. Substitution into (6) then gives

$$\omega(k \rightarrow 0) = \omega_p(k) \left[1 - \left[0.175 + \frac{0.0594}{\Gamma} - \frac{0.1109}{\Gamma^{3/4}} \right] ka \right] \quad (10)$$

for $\sqrt{2} < \Gamma < 50$ and

$$\omega(k \rightarrow 0) = \omega_p(k) \left[1 - \left[0.171 - \frac{0.154}{\Gamma} \right] ka \right] \quad (11)$$

for $\Gamma > 30$.

With increasing k , $\mathcal{D}(\mathbf{k})$ reaches a minimum and $\omega(k)$ increases to maximum; their values as $\Gamma \rightarrow \Gamma_m$ are

$$\left. \begin{aligned} \mathcal{D}_{\min} &= -0.5226 \\ \omega_{\max} &= 0.874\omega_0 \end{aligned} \right\} \text{at } ka = 1.60. \quad (12)$$

Thereafter, $\omega(k)$ descends through a series of oscillations to an asymptotic value. The wave-number position k_s of the first minimum in $\omega(k)$ (which, incidentally, is the lowest minimum) decreases asymptotically and reaches the value $k_s \sim 3.7/a$ at $\Gamma = 120$; at this Γ value, the spacing between successive minima is $\sim 3.7/a$. This is close

to the lattice spacing $K_0=3.3/a$ in the reciprocal lattice.¹⁵

The asymptotic value of $\omega(k \rightarrow \infty, \Gamma)$ is determined by

$$\mathcal{D}(k \rightarrow \infty) \rightarrow -1 - \frac{1}{4\pi k} \int_0^\infty dq q^2 g(q), \quad (13)$$

whence,

$$\omega^2(k \rightarrow \infty, \Gamma) = -\frac{1}{4}\omega_0^2 \int_0^\infty dx x^2 ng(x), \quad x=qa. \quad (14)$$

The right-hand side integral is bounded and we find that

$$\int_0^\infty dx x^2 ng(x) = -1.46$$

and

$$\mathcal{D}(k \rightarrow \infty) = -1 + \frac{0.365}{ka} \quad (15)$$

for $\Gamma > 90$. In the $k \rightarrow \infty$ limit the plasma mode is dominated by the individual particle motions which are therefore characterized by the plasmon frequency

$$\omega(k \rightarrow \infty) = 0.604\omega_0 \quad (16)$$

for $\Gamma > 90$.

It is interesting to analyze the lowest minimum at k_s , $\omega(k_s) \equiv \omega_s$, as a function of Γ ; it is a monotonically decreasing function reaching $\omega_s \approx 0.44\omega_0$ at $\Gamma = \Gamma_m$. Further increase of Γ may lead into a supercooled or glassy state. Extrapolation from the $\Gamma = \Gamma_m$ behavior indicates, however, that $\omega_s(\Gamma \rightarrow \infty)$ reaches the asymptotic value $\omega_s^* = 0.42\omega_0$; thus ω_s [and hence $\omega(k)$] is always greater than zero and no softening of the plasmon mode [$\omega^2(k) \leq 0$] occurs either for $\Gamma < \Gamma_m$ or for $\Gamma > \Gamma_m$. (See Fig. 2.)

To assess the accuracy of the present theory, we compare our dispersion curves for $\Gamma=7.07$, 22.36, and 50 with the Totsuji-Kakeya MD data¹ taken at about the same Γ values, and for the entire available range of wave numbers. Figs. 3(a)–3(c) show that as Γ increases, the comparison becomes more and more favorable, as it should. At $\Gamma=7.07$, the theoretical curve falls somewhat below the MD data for ka values between about 0.8 and 1.9. At $\Gamma=22.36$, the theoretical curve lies right on top of the MD data for ka values up to about 1.3. Beyond that and up to the $ka \approx 2.3$ limit of the experiment, the theoretical curve still falls somewhat below the experimental data. At $\Gamma=50$, however, the agreement between theory and computer experiment is quite good up to the $ka \approx 2.3$ limit of the experiment.

III. PLASMON DISPERSION WITH DIRECT THERMAL EFFECT INCLUDED

In addition to the “indirect” thermal effect encountered through the temperature dependence of the correlation function, the particles in the liquid state undergo a slow change of the position of their equilibrium quasites, which can be referred to as the “direct” thermal effect. The theory provided in paper I and employed in the preceding section ignores this effect, which becomes less and less significant as Γ increases towards Γ_m . However, the influence of the thermal migration on the dispersion is expected to be of the order kv_{direct} and therefore can become reasonably significant for intermediate- Γ and high- k values.

At the present time we have no *ab initio* approach to incorporate the direct thermal effect into the theory.

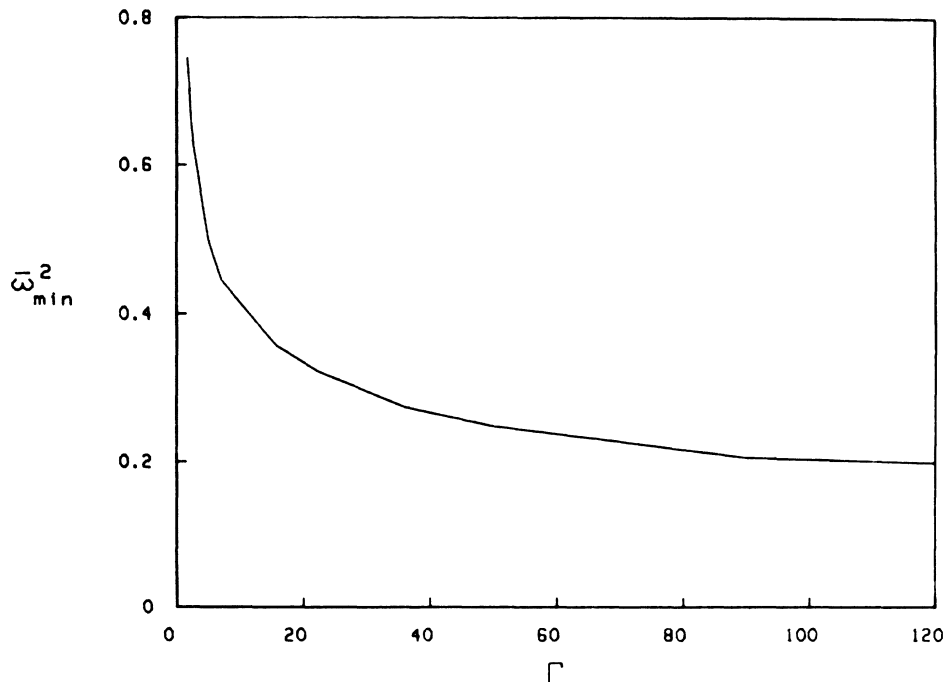


FIG. 2. ω_s^2 vs Γ ; $\bar{\omega}_s^2$ is the lowest minimum in $\bar{\omega}^2(\bar{k})$ at $\bar{k} = \bar{k}_s$; from Eq. (6), $\bar{\omega}_s^2 = \bar{\omega}^2(\bar{k}_s, \Gamma) = \bar{k}_s^2 [1 - \mathcal{D}_{\min}(\bar{k}_s, \Gamma)]$; $\bar{\omega} = \omega/\omega_0$, $\bar{k} = ka$, where $\omega_0 = (2\pi ne^2/ma)^{1/2}$ and $a = 1/(\pi n)^{1/2}$.

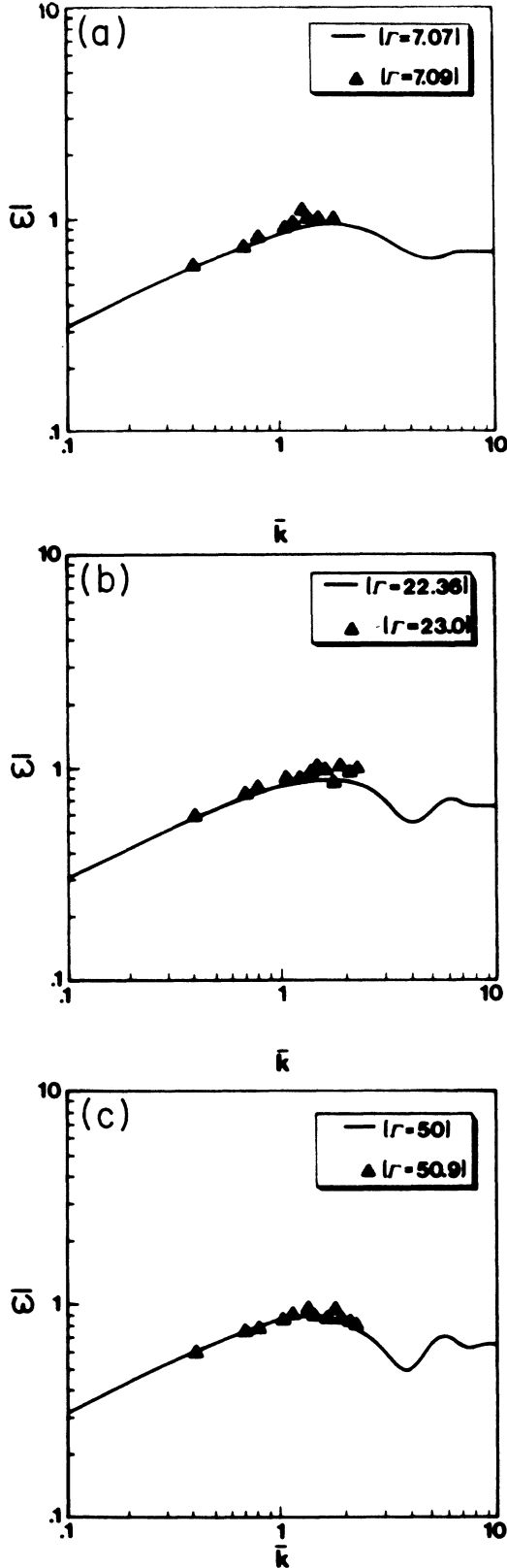


FIG. 3. Comparison between the Eq. (6) plasmon dispersion curves (solid line) and the MD data of Totsuji and Kakeya (Ref. 1) (triangular data points) for $\Gamma = 7.07, 22.36,$ and 50 ; $\bar{\omega} = \omega/\omega_0$, $\bar{k} = ka$, where $\omega_0 = (2\pi n e^2 / ma)^{1/2}$ and $a = 1/(\pi n)^{1/2}$.

However, a phenomenological treatment, through the reformulation of the dielectric function $\epsilon(\mathbf{k}\omega)$, can be carried through. There is, of course, no unique prescription for the phenomenological construction of $\epsilon(\mathbf{k}\omega)$. There are, however, certain criteria whose satisfaction is expected.

(i) In the $k \rightarrow 0$ limit, (1) should be recovered.

(ii) The ω^{-4} high-frequency sum rule—including the hitherto neglected thermal contribution—[see Eq. (4)] should be satisfied.

(iii) In the static ($\omega = 0$) limit, the perfect screening condition $\alpha(k \rightarrow 0, 0) \equiv \epsilon(k \rightarrow 0, 0) - 1 \rightarrow +\infty$ for sufficiently low Γ values and the compressibility sum rule [given by Eqs. (24) and (25) below] should be satisfied. [Note that the perfect screening condition is violated by (1). As to the compressibility rule, (1) provides, as already noted, a compressibility sum rule coefficient which is always negative.]

(iv) In the $\Gamma \rightarrow 0$ limit, $\alpha(\mathbf{k}\omega) = \alpha_0(\mathbf{k}\omega)$ [$\alpha_0(\mathbf{k}\omega)$ is the RPA polarizability] should be recovered.

A further input is provided by recalling that in the theory of the correlated electron gas, the concept of “local field correction” turned out to be very profitable; this requires the structure

$$\alpha = \frac{\alpha_0}{1 - \alpha_0 G}$$

where G is the correlation-induced local field correction. The structure we suggest now follows from the identification $G \rightarrow -\mathcal{D}$, providing the mean-field-theory formula

$$\epsilon(\mathbf{k}\omega) = 1 + \frac{\alpha_0(\mathbf{k}\omega)}{1 + \alpha_0(\mathbf{k}\omega)\mathcal{D}(\mathbf{k})} \quad (17)$$

for the dielectric response function; the 2D RPA polarizability is given by

$$\alpha_0(\mathbf{k}\omega) = \frac{\kappa}{k} \left[1 + i\sqrt{\pi} \frac{\omega}{k} \left[\frac{\beta m}{2} \right]^{1/2} W \left[\frac{\omega}{k} \left[\frac{\beta m}{2} \right]^{1/2} \right] \right], \quad (18)$$

where

$$W(z) = \frac{i}{\pi} \int_{-\infty}^{\infty} du \frac{e^{-u^2}}{z - u + i0} = e^{-z^2} \left[1 + \frac{2i}{\sqrt{\pi}} \int_0^z dt e^{t^2} \right] \quad (19)$$

is the plasma dispersion function. As to the criteria listed above, we see that (i) is obviously satisfied since $\alpha_0(k=0, \omega) = -\omega_p^2(k)/\omega^2$ and at long wavelengths, (17) becomes

$$\epsilon(k \rightarrow 0, \omega) = 1 - \frac{\omega_p^2(k)}{\omega^2} - \frac{\omega_p^4(k)}{\omega^4} \left[3 \frac{ka}{2\Gamma} + \mathcal{D}(k \rightarrow 0) \right] \quad (20)$$

where $\mathcal{D}(k \rightarrow 0)$ is given by (7) and the presence of the fa-

miliar $3ka/2\Gamma$ Bohm-Gross thermal term is to be noted. At short wavelengths, we observe from (15) that

$$\epsilon(k \rightarrow \infty, \omega) = 1 + \frac{\kappa}{k - \kappa} \simeq 1 + \frac{\kappa}{k}, \quad (21)$$

which differs markedly from the large- k behavior exhibited by (1).

Concerning criterion (iii), in the static limit and at long wavelengths ($k \rightarrow 0$), Eq. (17) becomes

$$\epsilon(k \rightarrow 0, 0) = 1 + \frac{\kappa_{\text{MFT}}}{k}, \quad (22)$$

$$\kappa_{\text{MFT}} = \frac{\kappa}{1 + \frac{5}{8}(\beta E_c/n)}, \quad (23)$$

guaranteeing satisfaction of the perfect screening condition for sufficiently low- Γ values. Comparison of (22) and (23) with the exact expression dictated by the compressibility sum rule

$$\epsilon(k \rightarrow 0, 0) = 1 + \frac{\kappa_{\text{exact}}}{k}, \quad (24)$$

$$\begin{aligned} \kappa_{\text{exact}} &= \kappa [\beta (\partial P / \partial n)_\beta]^{-1} \\ &= \kappa \left[1 + \frac{1}{2} \frac{\beta E_c}{n} + \frac{n}{2} \left[\frac{\partial}{\partial n} \frac{\beta E_c}{n} \right]_\beta \right]^{-1}, \end{aligned} \quad (25)$$

demonstrates the obvious structural similarity but at the same time a deviation from the required precise numerical value. In the $\Gamma \gg 1$ domain, the deviation, however, is not very significant. Substitution of (8), for example, into (23) and (25) gives

$$\kappa_{\text{MFT}} = \frac{\kappa}{-0.7\Gamma + 0.444\Gamma^{1/4} + 0.7625}, \quad (26)$$

$$\kappa_{\text{exact}} = \frac{\kappa}{-0.84\Gamma + 0.399\Gamma^{1/4} + 0.81}. \quad (27)$$

We also note that the high- k behavior of $\epsilon(\mathbf{k}0)$ is, in view of (21), quite satisfactory in reestablishing the screening property of the individual particle-like behavior. Finally at the dynamic level [criterion (ii)], one can readily verify that at high frequencies Eq. (17) reproduces the correct sum rule expansion (4) through $O(1/\omega^4)$ and for arbitrary k values. We can conclude that (17) certainly provides a satisfactory dielectric function for $\Gamma \gg 1$ —and probably a reasonable interpolation formula for arbitrary Γ —over the entire frequency and wave-number domain. It also preserves the good qualities of our original approximation scheme, in particular, the agreement with the phonon dispersion relation of the 2D Wigner crystal^{7,10} for $\Gamma \rightarrow \Gamma_m$. To the best of our knowledge, only the present theory and the theory of Ref. 7 can claim this kind of accuracy.

Now, from Eq. (17), the dispersion relation $\epsilon'(\mathbf{k}\omega) \equiv \text{Re}\epsilon(\mathbf{k}\omega) = 0$ can be written as

$$\frac{2\Gamma}{ka} \left[1 - \sqrt{\pi} \frac{\omega}{k} \left[\frac{\beta m}{2} \right]^{1/2} W'' \left[\frac{\omega}{k} \left[\frac{\beta m}{2} \right]^{1/2} \right] \right] \times [1 + \mathcal{D}(\mathbf{k})] = -1 \quad (28)$$

under the usual assumption that the imaginary part of the RPA polarizability is much smaller than its real part ($W'' \equiv \text{Im}W$).

For $k \rightarrow 0$, Eq. (28) simplifies to the long-wavelength plasmon dispersion relation

$$\omega(k \rightarrow 0) = \omega_p(k) \left[1 + \left[\frac{3}{4\Gamma} + \frac{5}{32} \frac{\beta E_c}{n\Gamma} \right] ka \right], \quad (29)$$

which, when combined with the data of Refs. 12 and 14, gives

$$\omega(k \rightarrow 0) = \omega_p(k) \left[1 - \left[0.175 - \frac{0.6906}{\Gamma} - \frac{0.1109}{\Gamma^{3/4}} \right] ka \right] \quad (30)$$

for $\sqrt{2} < \Gamma < 50$ and

$$\omega(k \rightarrow 0) = \omega_p(k) \left[1 - \left[0.171 - \frac{0.904}{\Gamma} \right] ka \right] \quad (31)$$

for $\Gamma > 30$. Equations (30) and (31) are slightly different from their Sec. II counterparts (10) and (11). We note the near-perfect agreement between the Bonsall-Maradudin formula¹⁰

$$\omega(k \rightarrow 0) = \omega_p(k)(1 - 0.172ka) \quad (32)$$

for the dispersion of longitudinal phonon excitations in the 2D Wigner lattice and the $\Gamma \rightarrow \infty$ limit of our plasmon dispersion formulas (11) and (31).

Equation (28) has been solved numerically for arbitrary k values with the same $g(r)$ data [given by the Monte Carlo (MC) simulations of Refs. 12 and 13 and by the Ref. 13 HNC calculations] as in the preceding section. The new dispersion curves $\omega(k)$ are displayed in Fig. 4. The inclusion of direct thermal effects into this extended model of the 2D OCP liquid has three consequences.

(i) The dispersion $\omega(k)$ is no longer oscillatory; rather, it exhibits a single maximum and then cuts off beyond that at the value $k = k_{\text{max}}(\Gamma)$ (see also Fig. 5); k_{max} increases with increasing Γ to the asymptotic value $k_{\text{max}}^* \sim 3.65/a$ at $\Gamma = 120$; note how close k_{max}^* is to the lattice spacing $K_0 = 3.3/a$ in the reciprocal lattice.¹⁵ Note also the coincidence between the value of k_{max}^* and the k value where the first minimum in $\omega(k)$ occurs in the $\Gamma = 120$ dispersion curve without the direct thermal effect [Fig. 1(b)].

(ii) Direct thermal effects markedly increase the $\omega(k)$ values and lead them to a higher maximum, especially at the lower coupling values.

(iii) Qualitatively similar to the RPA dispersion curve, the present dispersion curve is also divided into two branches at $k = k_{\text{max}}$: the upper branch corresponds to the plasmon branch and the lower branch is related to a soundlike mode with phase velocity somewhat higher (~ 1.24 – 1.38 times higher) than the electron thermal velocity; this latter branch is, however, heavily (Landau) damped and of no physical significance.

To assess the accuracy of this section's dispersion calculations, we again compare the (Fig. 4) dispersion curves for $\Gamma = 7.07, 22.36,$ and 50 with the Totsuji-Kekeya MD

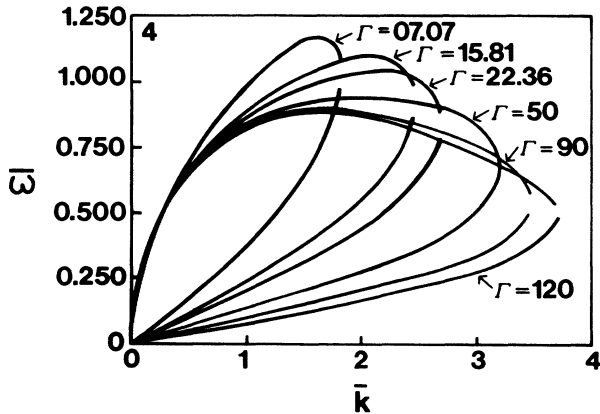


FIG. 4. Plasmon dispersion calculated from Eq. (28) for $\Gamma=7.07, 15.81, 22.36, 50, 90,$ and 120 ; $\bar{\omega}=\omega/\omega_0$, $\bar{k}=ka$, where $\omega_0=(2\pi n e^2/ma)^{1/2}$ and $a=1/(\pi n)^{1/2}$.

data¹ corresponding to these coupling values. Figures 6(a)–6(c) again show how the comparison becomes more and more favorable with increasing Γ as it should. At $\Gamma=7.07$, the theory curve lies somewhat above the MD data in contrast to what was stated in Sec. II. At $\Gamma=22.36$, the theory curve and data very nearly coincide up to $ka \sim 1$. Beyond that, the theory curve lies somewhat above the MD data. At $\Gamma=50$, the coincidence between theory and computer experiment now extends out to $ka \sim 1.6$. Beyond that, the theory curve is slightly higher. One additional observation: the $k_{\max}a$ values marking the cutoff of the theoretical dispersion curves appear to be close to the $ka \sim 2.3$ limit of the MD experiments—at least for $\Gamma=7.07$ and 22.36 ; for $\Gamma=50$, the $k_{\max}a \sim 3.2$ cutoff is somewhat higher. No conclusion can be drawn, however, from what could be a fortuitous coincidence.

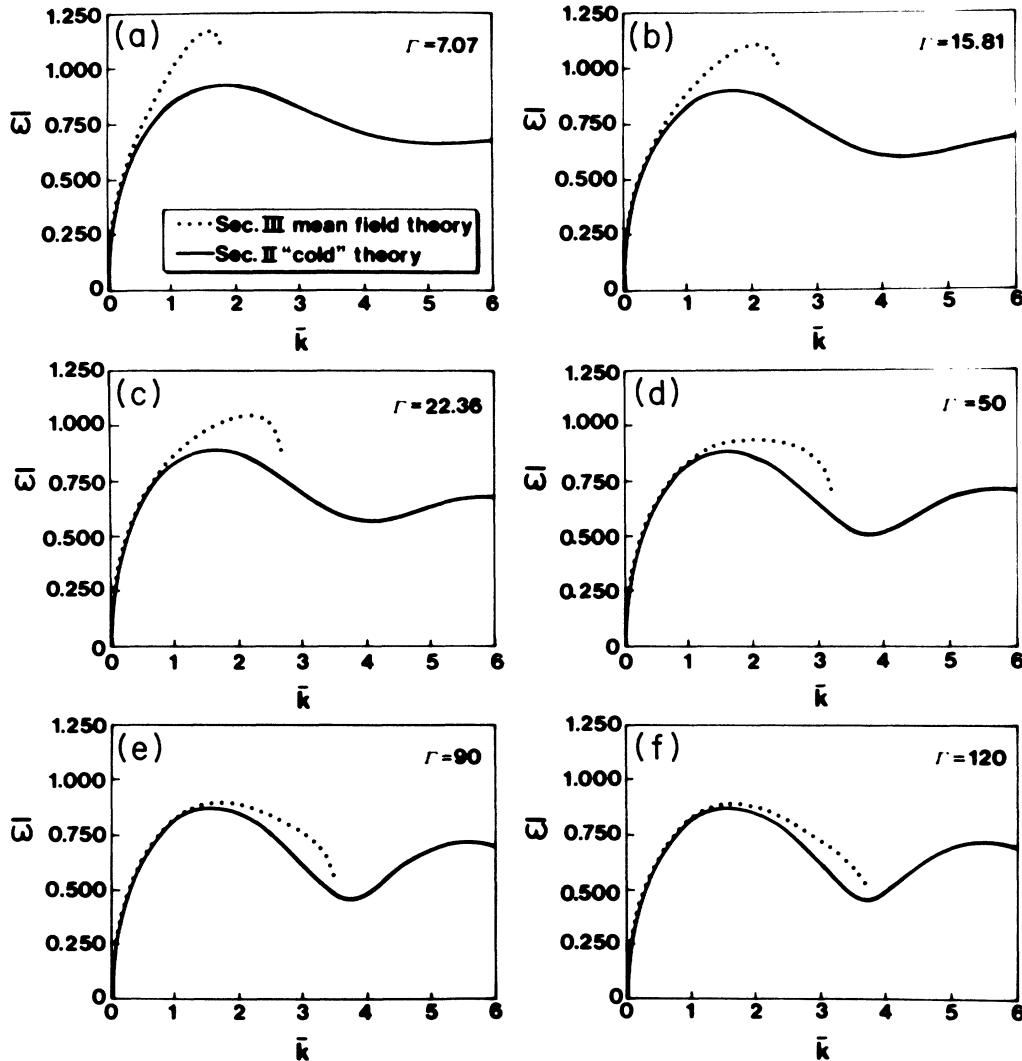


FIG. 5. Comparison between Eq. (6) (solid line) and Eq. (28) (dotted line) plasmon dispersion curves for $\Gamma=7.07, 15.81, 22.36, 50,$ $90,$ and 120 . Note how \bar{k}_{\max} corresponding to (28) approaches \bar{k}_s corresponding to (6) as $\Gamma \rightarrow \Gamma_m$; $\bar{\omega}=\omega/\omega_0$, $\bar{k}=ka$, where $\omega_0=(2\pi n e^2/ma)^{1/2}$ and $a=1/(\pi n)^{1/2}$.

IV. CONCLUSIONS

In this paper we have calculated the dispersion of the plasmon mode in the strongly coupled 2D OCP with $1/r$ interaction. Our analytical and numerical calculations were carried out at finite wave numbers and over a range of liquid-state coupling strengths up to $\Gamma = \beta e^2/a = 120$.

The starting point for these calculations was our formula (1) for the dielectric response function $\epsilon(\mathbf{k}\omega)$ which we derived in Ref. 1. In hindsight, Eq. (1) can be rewritten in the mean-field-theory-like form

$$\epsilon(\mathbf{k}\omega) = 1 - \frac{\phi(k)\chi_0(\mathbf{k}\omega)}{1 - \phi(k)\chi_0(\mathbf{k}\omega)\mathcal{D}(\mathbf{k})}, \quad (33)$$

where

$$\chi_0(\mathbf{k}\omega) = -\frac{1}{m} \int d^2v \frac{\mathbf{k} \cdot \frac{\partial}{\partial \mathbf{v}} F^0(\mathbf{v})}{\omega - \mathbf{k} \cdot \mathbf{v} + i0} \quad (34)$$

is the density-density response function of the system of noninteracting electrons, $\phi(k) = 2\pi e^2/k$ is the Fourier transform of the 2D Coulomb potential, and $\mathcal{D}(\mathbf{k})$ is given by (2). Equation (1) is then readily recovered by considering the electrons to be "cold" particles, viz.,

$$F^0(\mathbf{v}) = n\delta(\mathbf{v}), \quad (35)$$

whence

$$\chi_0(\mathbf{k}\omega) = nk^2/m\omega^2. \quad (36)$$

This is tantamount to neglecting the direct thermal effect (due to the slow migration of the quasites) against correlational effects in the response, which is precisely what we did in paper I. Equation (1) and its corresponding dispersion relation (6), however, certainly do not describe "cold plasma" oscillations, since the important effect of the temperature (through Γ) on the ensemble averaged quasiequilibrium background is well represented in the model by the equilibrium pair correlation functions comprising $\mathcal{D}(\mathbf{k})$. In Sec. III, the introduction of the direct thermal effect into the model is tantamount to replacing (35) with the 2D Maxwellian distribution

$$F^0(\mathbf{v}) = (\beta mn/2\pi) \exp(-\beta m v^2/2),$$

whence

$$\chi_0(\mathbf{k}\omega) = -\alpha_0(\mathbf{k}\omega)/\phi(k),$$

leading to the mean-field-theory formula (17) with $\alpha_0(\mathbf{k}\omega)$ given by (18).

At small wave numbers ($k \rightarrow 0$), the 2D OCP plasmon dispersion is described by Eqs. (10), (11), (30), and (31). At very strong coupling ($\Gamma \gg 1$), Eqs. (11) and (31) very nearly reproduce the definitive Bonsall-Maradudin formula (32) for the long-wavelength dispersion of longitudinal phonon excitations in the 2D OCP hexagonal lattice.

At finite wave numbers and in the absence of direct thermal effects (due to the slow migration of the quasites), the plasmon frequency $\omega(k)$ increases with increasing k from zero to a maximum whose value as $\Gamma \rightarrow \Gamma_m$ is given by (12). Thereafter, $\omega(k)$ descends

through a series of oscillations to a coupling-dependent asymptotic value given by (14). The oscillations become more and more pronounced with increasing Γ which is to be expected. The wave-number position k_s of the first

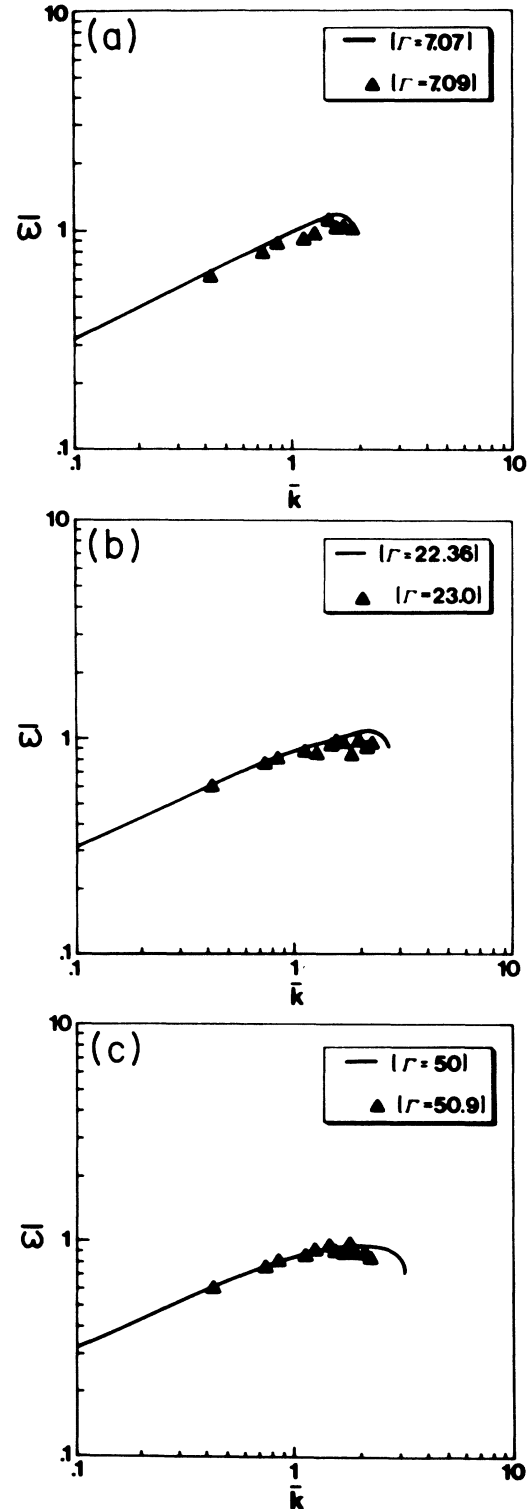


FIG. 6. Comparison between the Eq. (28) plasmon dispersion curves (solid line) and the MD data of Totsuji and Kakeya (Ref. 1) (triangular data points) for $\Gamma = 7.07, 22.36,$ and 50 ; $\bar{\omega} = \omega/\omega_0$, $\bar{k} = ka$, where $\omega_0 = (2\pi n e^2/m a)^{1/2}$ and $a = 1/(\pi n)^{1/2}$.

minimum in $\omega(k)$ decreases asymptotically and reaches the value $k_s \sim 3.7/a$ at $\Gamma=120$; at this value, the spacing between successive minima is approximately $3.7/a$ —close to the lattice spacing $K_0=3.3/a$ in the reciprocal lattice. In the presence of the direct thermal effect, the plasmon dispersion is almost entirely unaffected for $ka \leq 1$. Nevertheless, some rather dramatic changes in the dispersion do occur: (i) the dispersion is no longer oscillatory; rather, it exhibits a single maximum and then cuts off beyond that at the value $k=k_{\max}(\Gamma) < K_0$; k_{\max} increases with increasing Γ to the asymptotic value $k_{\max}^* \sim 3.7/a$ at $\Gamma=120$; the coincidence between the value of k_{\max}^* and the k value where the first minimum in $\omega(k)$ occurs in the $\Gamma=120$ “cold” dispersion curve is especially noteworthy [see Fig. 5(f)]; (ii) for $ka > 1$, the plasmon frequency is markedly increased especially at the lower coupling values; (iii) the dispersion curve now exhibits two branches: the upper branch corresponds to the plasmon mode and the lower branch corresponds to a soundlike mode with phase velocity somewhat higher than the electron thermal velocity.

We have compared our dispersion curves for $\Gamma=7.07$, 22.36, and 50 with MD data corresponding to these cou-

pling values [see Figs. 3(a)–3(c) and 6(a)–6(c)]. The comparison becomes more and more favorable with increasing Γ as it should. At $\Gamma=50$, the comparison is very good indeed.

We close by noting that Eqs. (1) and (17) should provide reliable descriptions of plasmon dispersion not only in the strongly coupled 2D OCP liquid states considered in the present work ($\Gamma < \Gamma_m = 137 \pm 15$), but also in the conjectured supercooled and amorphous glassy states which might exist for $\Gamma > \Gamma_m$. The existence of these latter states in two dimensions, however, has yet to be explored. In any case, continuation of dispersion calculations based on Eqs. (6) and (28) into the $\Gamma > \Gamma_m$ coupling regime is contingent on the availability of $g(r)$ data from future MC computer experiments and/or HNC calculations.

ACKNOWLEDGMENTS

This work has been partially supported by the National Science Foundation, Grant Nos. ECS-8713337 and ECS-8713628.

*Present address: Hewlett-Packard, Colorado Integrated Circuits Division, M.S. 64, 3404 East Harmony Rd., Fort Collins, CO 80525.

¹H. Totsuji and N. Kakeya, *Phys. Rev. A* **22**, 1220 (1980).

²H. Totsuji, *J. Phys. Soc. Jpn.* **40**, 857 (1976).

³De-xin Lu and K. I. Golden, *Commun. Theor. Phys. (Beijing, China)* **4**, 21 (1985).

⁴P. M. Platzman and N. Tzoar, *Phys. Rev. B* **13**, 3197 (1976).

⁵N. Studart and O. Hipolito, *Phys. Rev. A* **22**, 2860 (1980).

⁶K. S. Singwi, M. P. Tosi, R. H. Land, and A. Sjolander, *Phys. Rev.* **176**, 589 (1968); K. S. Singwi, A. Sjolander, M. P. Tosi, and R. H. Land, *Solid State Commun.* **7**, 1503 (1969); *Phys. Rev. B* **1**, 1044 (1970).

⁷K. I. Golden and De-xin Lu, *Phys. Rev. A* **31**, 1763 (1985).

⁸K. I. Golden and G. Kalman, *Phys. Rev. A* **19**, 2112 (1979).

⁹C. C. Grimes and G. Adams, *Phys. Rev. Lett.* **42**, 795 (1979).

¹⁰L. Bonsall and A. A. Maradudin, *Phys. Rev. B* **15**, 1959 (1977).

¹¹G. Kalman and K. I. Golden, *Phys. Rev. A* **41**, 5516 (1990).

¹²H. Totsuji, *Phys. Rev. A* **17**, 399 (1978).

¹³R. C. Gann, S. Chakravarty, and G. V. Chester, *Phys. Rev. B* **20**, 326 (1979).

¹⁴F. Lado, *Phys. Rev. B* **17**, 2827 (1978).

¹⁵P. M. Platzman and H. Fukuyama, *Phys. Rev. B* **10**, 3150 (1974).